Final Report

Project Title:	Theoretical design and discovery of the most-promising, previously overlooked hybrid perovskite compounds
Project Period:	05/01/16 – 12/31/17
Project Budget:	$250,000
Submission Date:	02/01/2018
Recipient:	Alex Zunger,
Address:	RASEI, 4001 Discovery Dr, Boulder, CO 80303
Award Number:	DE-EE0007366
Project Team:	A. Zunger, L.L. Kazmerski, G. M. Dalpian
Contacts:	Cheryl Brazeau cheryl.brazeau@colorado.edu 303-665-2742 Cell: 720-581-2025

Executive Summary

The material class of hybrid organic-inorganic perovskites (AMX_3) has risen rapidly from a virtually unknown material in photovoltaic applications a short 8-years ago into 20-23% efficient thin-film solar cell devices. As promising as this class of materials is, however, there are limitations associated with its poor long-term stability, non-optimal band gap, and the presence of toxic Pb atom on the metalloid site. An Edisonian laboratory exploration (*i.e.*, growth + characterization) via trial-and-error processes of all other candidate materials, is unpractical. Our approach uses high speed computational design and discovery to screen the 'best of class" candidates based upon optimal functionalities.

Our **goal** is to explore this larger materials space and identify the most promising hybrid-perovskite compounds, so we do *not* overlook potentially stronger candidates and an unanticipated winner.

Our **objectives** and **research plan** have been divided into two-distinct phases, defined as:

Stage 1: To screen a group of ~100 candidates by theoretically selecting the optimal A-molecule, M-metalloid atom and X-halogen atom, overcoming: (i) instability problems and (ii) presence of toxic Pb, while (iii) optimizing the key materials properties (better match band gap and absorption to solar photons).

Stage 2: To study the defects in the top compounds to determine dopability (ability to introduce free-carriers in these materials, needed thin-film solar-cell material). As promising as this class of materials is, however, there for solar cells, without creating adverse structural defects), and (b) presence of any detrimental defects.

Within **'Stage 1'**, we have identified in this materials screening program 18 winning compounds from a materials space composed of ~100 candidates, including the most commonly used materials of $[CH_3NH_3]PbI_3$ and $[CH(NH_2)_2]PbI_3$. Of them 14 are Pb-free (including 5 Ge-based materials (i.e., CsGeI3, CsGeBr3), [NH3OH]GeBr3, $[NH_2NH_3]GeBr_3$, and $[CH_3NH_3]GeI_3$, and 9 Sn-based materials, i.e., $CsSnI_3$, $CsSnBr_3$, $CsSnCl_3$, $[CH_3NH_3]SnI_3$, $[CH_3NH_3]SnBr_3$, $[CH(NH_2)_2]SnI_3$, $[CH_3CH_2NH_3]SnI_3$, $[C(NH_2)_3]SnI_3$, and $[NH_2(CH_3)_2]SnI_3$), and 7 show substantially enhanced thermodynamic stability with respect to $[CH_3NH_3]PbI_3$ (i.e., $CsSnBr_3$, $CsSnCl_3$, $CsGeBr_3$, $[CH_3NH_3]SnI_3$, $[CH_3NH_3]SnBr_3$, $[CH_3CH_2NH_3]SnI_3$, and $[NH_2(CH_3)_2]SnI_3$).

For **'Stage 2'**, our defect calculations focused $CsSnI_3$, $CsSnBr_3$ and $CsSnCl_3$, and we HAVE found that they should be defect tolerant (i.e., do not present transition levels inside the band gap). Also, Sn vacancies have low-formation energies, becoming negative at energies slightly above the VBM. Because of this, they should be usually p-type semiconductors. Additionally, because of the interest and some uncertainties surrounding the defect data and calculations, we have started a discussion (blog) within the 'defects' community. This has added an unplanned benefit to our and the community research, stating best practices when performing defect calculations in solids, initiating collaborations and sharing within this segment of theoreticians and experimentalists, and bringing focus and collaboration among these groups.

Finally, we have had a priority in publishing/disseminating results and handing them

to EERE, the technology field, and the relevant experimental groups of our: (1) improved candidate PV materials, and (2) our proven high-payoff theoretical methodology as a resource for their materials & device development arsenal. We have attained our **expected outcome** of theoretical filtering of a few most promising candidate AMX3 compounds, for future to laboratory realization.

Table of Contents

1. Background

The family of hybrid organic-inorganic halide perovskites AMX_3 has recently become a rising star in the field of solar-energy materials, with the power conversion efficiency of thin-film small area photovoltaic (PV) solar cell based on this class of materials progressing rapidly from the initial value of 3.8% in the year 2009,[1] reaching an unprecedented (and unanticipated) high values, now exceeding 23% only a few years later[2,3,4]. Although limited to very small area research PV cells, such research-device efficiencies have become competitive with the record efficiencies of conventional crystalline Si, CdTe and Cu(In,Ga)Se_2 thin-film solar cells that have been studied for several decades. Furthermore, the hybrid perovskite can be potentially synthesized by the low-cost, room-temperature solution processing methods, projected to be large scale manufacturing compatible. Recent reports of high-efficiency tandem approaches with better stability have added to the interest in these devices.[5]

However, there are still a few challenges in this field. We will summarize three of these challenges, and comment on how our work helped advance these issues.

(i) It is highly desired to reduce the optical band gap of $(CH_3NH_3)PbI_3$ (1.51 eV) and $(CH_3NH_3)PbBr_3$ (2.35 eV) to the optimal value of 1.34 eV according to the Shockley–Queisser limit. Recent results from the McGehee group suggest that the use of cubic materials should help getting this band gap.[6] They also show that, by alloying the A, B and X sites, one can control parameters such as the crystal structure, the lattice parameter and the tilting of the octahedral, fine-tuning the bandgap;

(ii) The devices fabricated using the known materials show poor long-term stability under higher temperatures and outdoor illumination, as well as in the presence of moisture and/or oxygen. This may be attributed to the intrinsic thermodynamic instability of the materials discovered thus far. In a recent commentary in *Nature*,[7] Yang and You urged researchers to make perovskites more stable. Consequently, there are still several open issues regarding this very important point.

(iii) The use of Pb-containing materials is an environmental concern, being banned in commercial electronic devices and in consumer products in many markets worldwide. There have been some advances in this direction, mainly by substituting Pb by Sn or by creating 'double perovskite' materials. In this latter approach, the Pb^{2+} atoms are substituted by on +1-element and one +3-element. On average, the B site will still be 2+.[8] An interesting candidate for this kind of compounds is $Cs_2InAgCl_6$.[9]

The first part of our current research goes in the direction of addressing *all three points* above. We report on a comprehensive list of materials, that *meet all three criteria*. First, we focus on cubic perovskites that are ideal for the choice of bandgaps. Second, we report on the stability of each compound. And third, we report specifically on compounds that do *not* contain Pb atoms.

From the perspective of defects and dupability (defined as the ability to create and control free carriers), highly needed to tune the properties of the solar cells, it is believed that halide perovskites are 'defect tolerant',[10] (i.e., without the existence of deep trap

levels inside the band gap).[11] This fact has been acknowledged by a large part of the community, although there is still no clear consensus. Different theoretical studies report very different sets of results, with differences in the population of defects and the existence or not of deep trap levels.[12] Part of the community blames computational details for the difference in results (spin-orbit coupling and band gap corrections). A major problem related to this fact is the absence of detailed description of the exact technical details of the respective calculations; something that severely hampers the reproducibility of the published data.

Our project fits within the current literature in the sense that we have reported the basic properties of all cubic perovskites, and because we are working in the direction of setting the best practices when performing defect calculations in semiconductors and insulators. This will become clear in the development of this report.

2. Introduction

We have proceeded with this research project with the strongly held the opinion that it is better to select materials for technology based on *microscopic understanding of the limiting factor*s, rather than based on a shotgun combinatorial attempt to make all and test all. Historical examples of poorly understood material instability that came back years later to haunt the technology include the Staebler-Wronski instability in amorphous silicon, or the "dark spots" instability in CdHgTe night-vision detectors. To select the best AMX_3 materials non- phenomenologically one needs to establish the critical, materials-specific *'design principles'* (DP's) that render such materials in solar cells superior. DP's refer to microscopic *physical understanding of mechanisms* that control the functionality at hand.

Considering these principles, the main goals of this project are to establish an understanding of

(i) Alternative halide perovskites

(ii) Stability, and (iii) role of defects and doping. In the first stage of the project, we've screened a group of ~100 candidates by theoretically selecting the optimal A-molecule, M-metalloid atom and X-halogen atom, overcoming: (a) instability problems and (b) presence of toxic Pb, while,

(iii) Optimizing the key materials properties (better match band gap and absorption to solar photons). In the second stage, we studied the defects in the top compounds to determine dopability (defined as the ability to introduce and control free-carriers in these materials).

3. Project Results and Discussion:

Our goal has to explore this larger materials space and identify the most promising hybrid perovskite compounds to ensure that we do not overlook potentially stronger candidates and an unanticipated winner. In this section, we address the research and tasks that has been completed for the 2 phases: Stage 1: to screen a group of ~100 candidates by theoretically selecting the optimal A-molecule, M-metalloid atom and X-halogen atom, overcoming: (i) instability problems and (ii) presence of toxic Pb, while (iii) optimizing the key materials properties (better match band gap and absorption to solar photons). And, Stage 2: to study the defects in the top compounds to determine (a) dopability (ability to introduce free-carriers in these materials, needed for solar cells, without creating adverse structural defects), and (b) presence of any detrimental defects.

We are using a **rational set of *functionality filters*** (FFs**) applied successively** to a group of ~100 candidate AMX_3 compounds, so that only compounds that have passed the "n^{th} FF are subjected to the **next** (n+1) FF test. This way we do not have to calculate ALL properties for ALL compounds (as practiced in 'high-throughput' approaches). The defined research tasks are:
Task 1.1 (Month 1) **Establish Materials Framework, Computational Methods, & Design Metrics**, test our computational science methodologies for these metrics, & establish our materials framework.
Task 1.2 (Months 1-6) **Apply the FF of thermodynamic stability to screen ~100 bulk hybrid perovskite** materials (eventually to expected ≤30) using the relevant decomposition enthalpy of reaction $AMX_3 \rightarrow AX + MX_2$ as a design metric and related stability tests. We have already identified that cubic $CH_3NH_3PbI_3$ is slightly thermodynamically unstable, and expect to find new hybrid perovskites that can be thermodynamically stable.
Task 1.3 (Months 2-9) Considering only the compounds that passed the stability test, **apply next set of FF's concerning electronic properties: band structure, optical absorption and effective masses.**
Task 1.4 (Months 6-12): Considering only compounds that have passed the stability test FF as well as the electronic properties FF, **perform extensive defect calculations seeking potentially defect tolerant systems to determine the "Best-of-Class" candidates that have desired and predicted stability, electronic properties, and defect-tolerance.**
Task 1.5 (Months 10-12): Hand off of the most promising (Best-of-Class) results to the appropriate groups for development.

We now describe the research accomplishments and results for each of these tasks.

Task 1.1 Establish Materials Framework, Computational Methods, & Design Metrics, test potential computer access on EERE system at NREL and validate results on one base AMX_3 compound (with respect to experiment). The metrics will include base thermodynamic stability, band gaps, effective masses and other relevant properties.
Outcome Task 1.1: Trained the new post doc Leonardo Abdalla in the basic codes and methodologies and an Academic visitor Prof. Gustavo Dalpian. Established computer link with

EERE computer at NREL and tested our band structure programs and defect codes successfully by reproducing published results on formation enthalpy of Pb-based AMX3.

Task 1.2 Apply the functionality of thermodynamic stability to screen ~100 bulk hybrid perovskite materials (eventually expected to be ≤30) using the (a) crystal structure and (b) decomposition enthalpy of reaction $AMX_3 \rightarrow AX + MX_2$ as a design metric for stability.

Outcome Task 1.2: Figure 1 summarized the results of screening ~ 100 new halide perovskites.

Understanding stability issues on the perovskites Research on halide perovskites has advanced a lot in the last few years, but stability issues are still a major concern. In a recent comment in Nature[7], Yang and You urge researchers to *"stop these promising photovoltaics from degrading"*. We found that the word "stability" or "instability" in this context is poorly defined. Our research revealed a few shades of stability:

(i) Stability of a single AMX_3 perovskite with respect to decomposition into other compounds ($AMX_3 \rightarrow AX+MX_2$) (see Figure 1 therein). We find that the Pb compounds are slightly unstable), whereas the Sn compounds are more stable in this respect. Calorimetric measurements have also found similar results, indicating the instability of the most famous Pb halide perovskite $MAPbI_3$.[13] This trend goes against the commonly articulated opinion that "Sn compounds are less stable than Pb compounds", but this is because the single word "unstable" does not convey the specific channel of instability. Sn compounds are less stable than Pb compounds in a completely different sense noted next.

(ii) The stability of AMX_3 compounds wrt oxidation, i.e., reactions like $2AMX_3 \rightarrow A_2M\square X_6 + M$. The Sn compounds are notorious in that they can easily lose Sn, forming Sn vacancies. In doing so, Sn that was Sn (II) is oxidized to Sn(IV). This process will lead to a whole new class of halide perovskites. An interesting candidate for this new 216-compound is Cs_2SnI_6. Once 113 compound AMX3 is oxidized to form the Ordered Vacancy Compound 216, the latter is no longer sensitive to oxidation as it's the 'end of the road' compound. Our calculated phase diagrams, using the new SCAN functional, have shown a smaller stable region for the stability of the 113 compounds. The formation energy of the Sn vacancies is very small, indicating that they should form almost spontaneously. This is a clear indication that, under Sn-poor, oxidizing conditions, the 216 compound is more stable. They have already been synthesized, as well as those based on Br and Cl.

(iii) The stability of the 113 and 216 Sn-based compounds with respect to deep recombination centers: Our *ab initio* calculations indicate that 113 compounds have favorable defect properties, i.e., are 'defect tolerant', while the 216 [14] present deep defect levels that are not favorable for PV applications (see results below). For the 216 compounds, the deep defect levels. We observed that, for $CsSnI_3$, vacancies are very likely to form when the material is subjected to a Sn-poor environment. This will make it easy to form the new compound Cs_2SnI_6, that is a Sn-deficient material when compared to the original one. Experimentally this compound is said to be more stable to moisture and oxidation. However, the new material will have deep levels in the band gap, not being suitable for PV applications. *This explains why the 216 compounds, despite being stable wrt channels (1) and (2) are limited as PV materials*.

(iv) Dynamic (phonon) instability with respect to phonons: We found to our surprise that some of the perovskite compounds including 216 have soft phonons in the cubic phase at low temperatures. This project is beyond the scope of this proposal. However, for the sake of completeness, we briefly mention it here. We have taken measured crystallographic data for Cs_2SnX_6 (X=Cl, Br and I) and performed phonon calculations on these structures. All them are cubic according to X-ray data. Our calculations show that some of these structures have negative phonons. This might mean two things: (i) they are not stable in the cubic structure and would transform to non-cubic phases; (ii) anharmonic effects might be important in this case rendering the structures stable but *at high temperatures.*

(v) Additional unplanned accomplishment (in collaboration with DOE office of Science): Does ASnX3 and A2SnX6 have different charges on Sn or not?

The halide perovskites $A^{I}M^{IVB}X^{VII}_3$) are successful as semiconducting *solar absorbers*, having band gaps as low as 1.2 eV for $CH_3NH_3SnI_3$ and 1.5 eV for $HC(NH_2)_2PbI_3$).This is surprising (although accepted without questioning...) given that they represent in essence **ionic metal halides** $A^+[(Pb/Sn)X_3]^-$. In contrast, the analogous compounds $A^+[Ba/SrI_3]^-$ where divalent Sn(IVB) s^2p^0 is replaced by Sr(IIA) have far larger band gaps (~ 4 eV for $CsSrI_3$), being insulators and useless as photovoltaic (PV) absorbers. We studied the reason for this finding. We find that we owe this special feature of PV-useful *small gaps formally ionic* $A^{I}M^{IVB}X^{VII}_3$ compounds to the fact that Sn shows a "self Regulating Response" whereby the physical charge on the Sn site in $ASn(II)X_3$ and on Sn in $A_2Sn(IV)X_6$ are similar even though the formal oxidation state has changed from Sn(II) s^2p^0 to Sn(IV) s^0p^0. These results were obtained in collaboration with experimentalists (C. Stoumpos and Mercury G. Kanatzidis from Northwestern University) that performed X-ray, Mossbauer and XANES measurements, together with our ab initio calculations. The implication is profound: Even though one removes 50 % of the Sn atoms from the 113 compound in forming the 216 compound, and naively thinking this should transform the remaining Sn in 216 to Sn(IV) (i.e., addition of two holes relative to 113), in reality the charge on Sn is hardly changed. This resistance to perturbations makes these compounds small gap relative to $CsSrI_3$ that behaves, unlike $CsSnI_3$, as a wide-gap ionic material.

Looking at the charge deformation map we can see the redistribution of charges. This is defined as $\Delta\rho = \rho^{113} - \rho^{216} - \rho^{Sn}$, where ρ^{113} and ρ^{216} refers to the total valence charge density of CsSnI3 and Cs2SnI6, respectively. ρ^{Sn} is the charge density of the sublattice of Sn that is removed, and is used to balance the total charge difference. By necessity we use a fixed geometry for all the components either in the lattice parameter of the 113, in Fig. 4a, or the lattice parameter of the 216 compound, as show in Fig. 6. Both cases give similar results. The position of the Sn atoms, Sn vacancies and I atoms are indicated and a density profile along a representative line (Fig. 4b) gives a better idea of the amplitude of the differences. Blue areas indicate negative values.

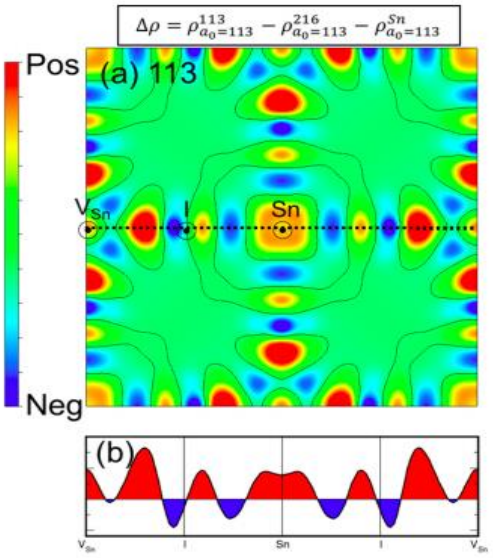

Figure 1. (a) Charge density difference map. The lattice parameter of the 113-compound was used as reference. The charge difference is displayed on the [001] plane containing Sn atoms, Sn vacancies, and I atoms. (b) Profile of the charge density difference along the dotted line marked in (a) shows the oscillation between charge accumulation and depletion as the function of distance away from the Sn atom. Red and blue areas denote positive and negative charge density difference, respectively.

When we go from the 113 to the 216 compounds there is a small but noticeable charge migration from the Sn atom to the Sn-I bond. The small change in the charge around the Sn atom corroborates that the charge sitting on the Sn atom is very similar for both compounds. Owing to the reconfiguration of charges away from the center of atoms, it is also clear that we move from a more ionic (113) to a more covalent (216) compound. We see how the SRR works – charge is redistributed into positive (red) and negative (blue) oscillating domains so that the perturbation in physical charge upon vacancy formation is minimal.

Besides the analysis of the charge redistributions, we were also able to observe the chemical trends of the bandgaps of these compounds as we change the halide atom from Iodine to bromine and to chlorine for both the 113 and for the 216, vacancy-ordered compound:

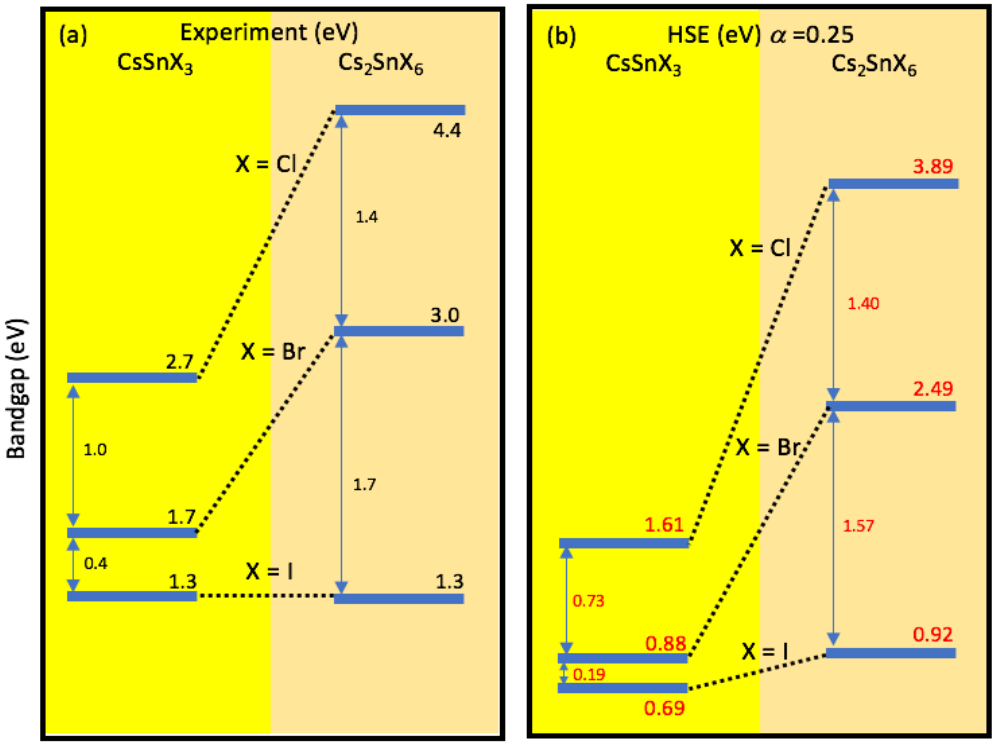

Figure 2: (a) measured bandgaps for 113 and 216 halides. (b) calculated bandgaps using density functional theory and hybrid exchange-correlation functional (α = 0.25). Experimental lattice parameters were used in the calculations.

Task 1.3: Considering only the compounds that passed the stability test, apply next set of functionality filters concerning electronic properties: band structure, optical absorption and effective masses**.**

Outcome of Task 1.3:

The figure below (Fig 3) (a) shows the constitution space of candidate $AM^{IV}X^{VII}_3$ perovskites for the materials screening, where ten cations were chosen for the A site, three group-IVA metalloids (Ge/Sn/Pb) for the MIV site, and three halogen (Cl/Br/I) anions for the X^{VII} site. Part (b) of the figure shows step-by-step screening process with the more and more DMs applied (different rows).Each column corresponds to one class of the 9 $AM^{IV}X^{VII}_3$ compounds with fixed A, whose arrangement coordinates are shown in the right panel. The red squares mean the materials passing the screening (Selected) and the gray ones mean the materials not passing (Abandoned). The last row of finally winning solar materials is highlighted.

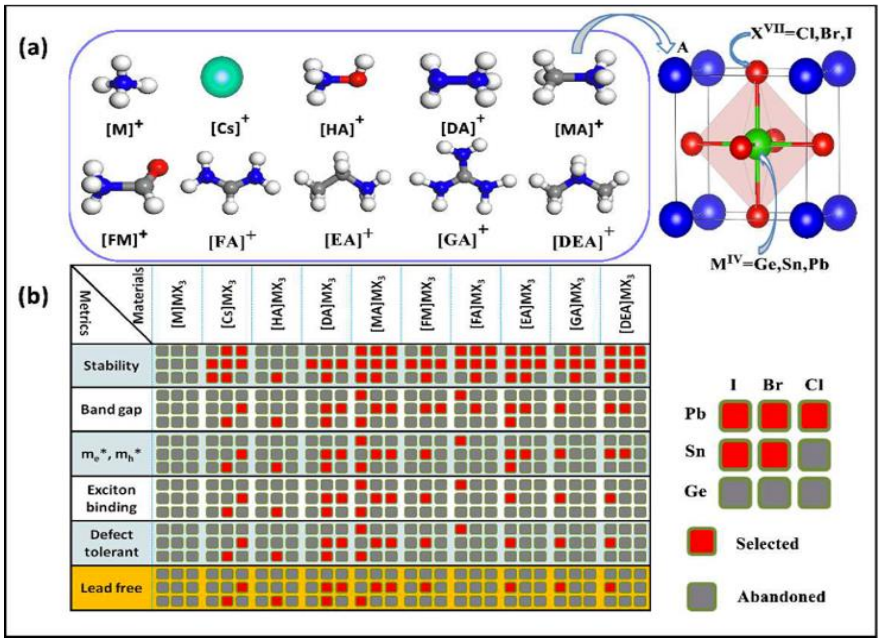

Figure 3. Representation showing how compounds are accepted(red) or rejected (grey) based on different functionality metrics**.**

Figure 4 shows the formation enthalpies reflecting thermodynamic stability, the decomposition enthalpy ΔH of $AM^{IV}X^{VII}_3$ perovskites [except for $AGeCl_3$]. The order of small molecules in the *x*-axis is sorted in terms of their steric size (i.e., r_A). Generally, one

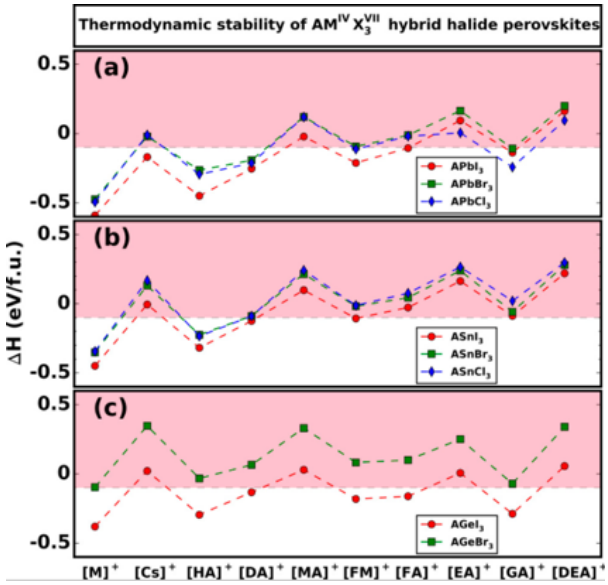

Figure 4. Calculated decomposition enthalpies ΔH of (a) Pb, (b) Sn, and (c) Ge based $AM^{IV}X^{VII}_3$ perovskites with respect to decomposed products of AM^{IV} + $M^{IV}X^{VII}_2$. Positive ΔH values mean no decomposition occurring. The compounds located in shaded area (with ΔH > -0.1 eV/f.u.) pass the materials screening.

observes a rather large span of ΔH (~1.0 eV). This indicates the thermodynamic stability

of this class of compounds depends strongly on the (A, M^{IV}, X^{VII}) combination. While for Pb (Figure 2a) and Sn (Figure 2b) based compounds the change of Δ*H* from chlorides to bromides to iodides is small, Ge based bromides exhibit the much stronger stability than that of iodides (Figure 4c). Walking through different cations at the A site, we find that four cations, i.e., Cs^+, MA^+, EA^+, and DEA^+, show evidently strong stability.

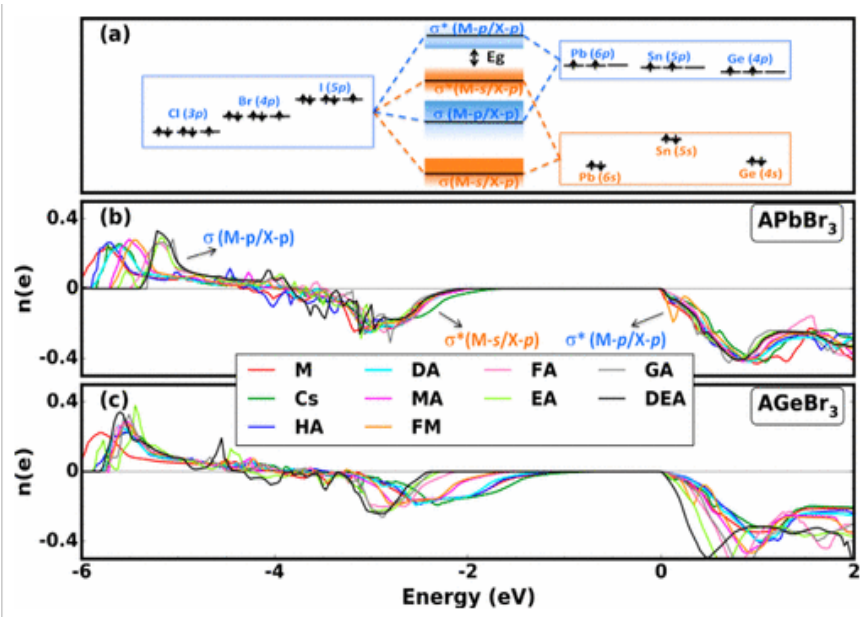

Figure. zzzzzzzzzzzzzzzzzzzzzzzzzzzzzzzzzzzzzzzzzzzzzzzzzzz

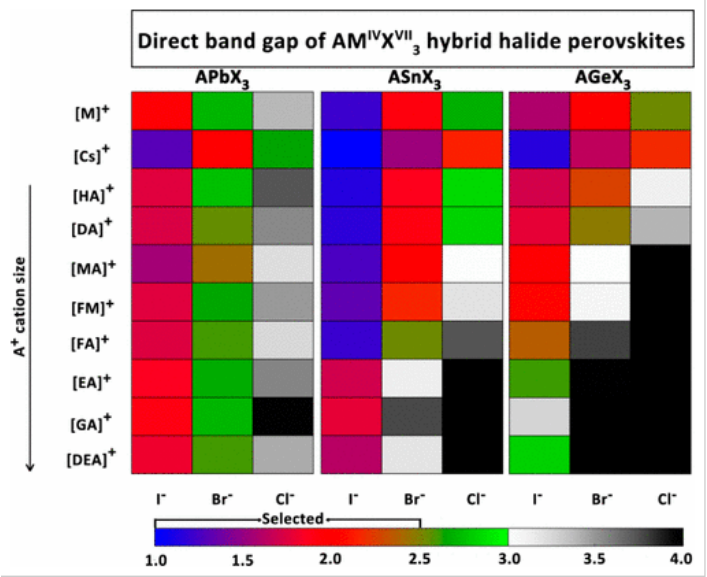

Figure 6. Calculated direct band gaps Egd of the AMIVXVII3 perovskites. The A+ cations are sorted by the increasing steric sizes. The gap values of 1.0–3.0 eV (promising for solar materials) are depicted by the RGB colors, and the oversized ones above 3.0 eV aredepicted in the RGB colors, and the oversized ones above 3.0 eV are shown in the White-black scale. The criterion of gaps smaller than 2.5eV is used for the materials screening.

Figure 6 shows calculated E_g^d of the $AM^{IV}X^{VII}_3$ perovskites, and Figure 5 depicts how the band gap is formed by various bonding/antibonding states that are characterized with the analysis of crystal orbital overlap population (COOP). There exists a wide distribution of gap values ranging from about 1.0 to 6.0 eV. This wide variation of E_g^d is attributed to (i) the energy difference between the X^{VII}–*p* orbital and the M^{IV}–*p*/*s* orbitals forming band-edge changes with different (M^{IV}, X^{VII}) combinations and (ii) the absolute positions of the CBM and the VBM, which are both antibonding states, being tuned by varied M^{IV}–X^{VII} bonding strengths (see Figure 4a). With increasing electronegativity of X^{VII}, the band gaps show significant enlargement, which is consistent with experimental observations. This makes the majority of the Pb-based and part of the Sn/Ge-based bromides and chlorides not favorable as solar materials owing to their too large E_g^d. The iodides family thus contains the most numerous optimal solar materials. Walking through different organic molecules, we found Pb-based compounds show weak dependence of E_g^d on A^+ cations, whereas Sn/Ge-based ones have dramatically increased $E_g^d$with increasing steric sizes of A^+. Taking the bromides as the instance, the E_g^d of Pb-based compounds varies within a relatively narrow energy range of 1.98–2.74 eV, but the E_g^d of Sn and Ge-based ones show the much wider tunability within the range of 1.53–3.77 eV and 1.64–4.15 eV, respectively. Since A^+ cations have no direct contribution to band-edge states, their influence on E_g^d is exerted though geometric modification of the M^{IV}–X^{VII} network composed of corner-sharing $M^{IV}X^{VII}_6$ octahedra.

One of the main factors in determining carrier mobility is the carrier effective mass. The effective masses were thoroughly calculated for all the available single perovskites. Figure 7 shows the results. Materials that have effective masses in between the shaded areas have passed the screening criterion ($m_e < 0.5\ m_0$ and $m_h < 0.5 m_0$).

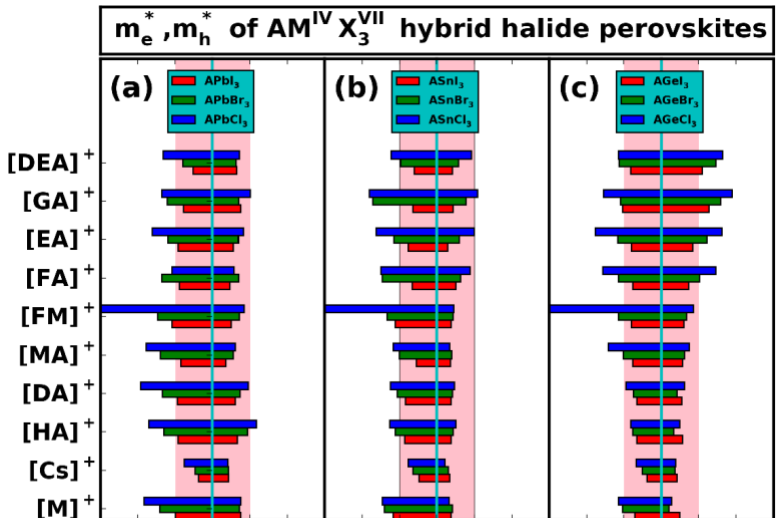

Figure 7. Calculated electron (m_e*, left panels) and hole (m_h*, right panels) effective masses of (a) Pb, (b) Sn, and (c) Ge based $AM_{IV}X_{VII3}$ perovskites. Shaded areas indicate the screening criterion applied (m_e* < 0.5 m0 and m_h* < 0.5 m_0).

We have also estimated the exciton binding energies of all calculated halide perovskites, as reported in Figure 6. Together with the numerical values reported in Figures 2, 3, 4 and 5 were used to produce figure 1, that gives our final view of the selected materials for this task.

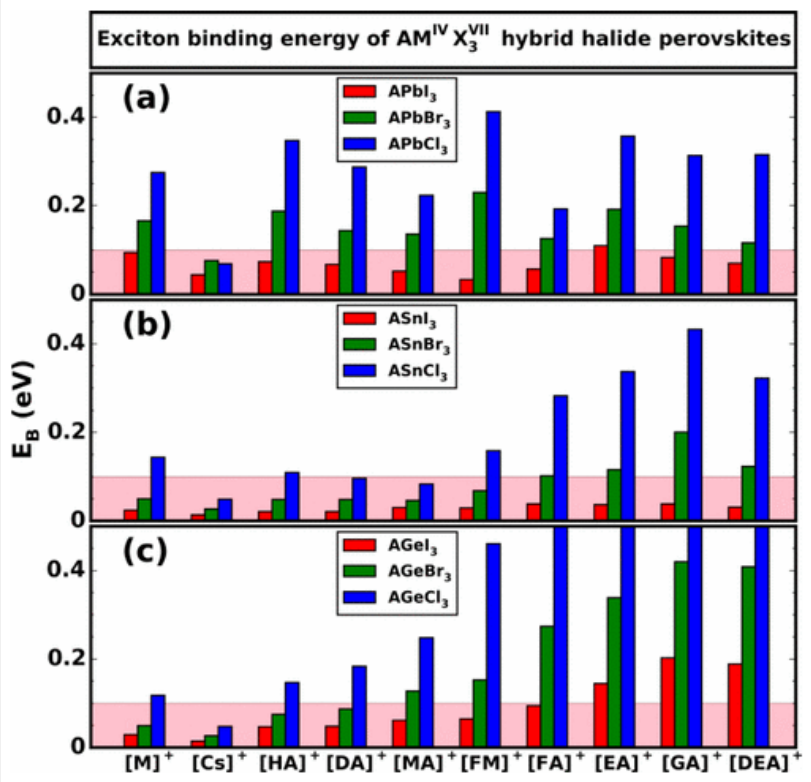

Figure 8. Calculated exciton binding energies of (a) Pb, (b) Sn, and (c) Ge based AMIVXVII3 perovskites with the hydrogen-like Wannier–Mott model. Shaded areas indicate the criterion applied (EB < 0.1 eV) for the materials screening.

Task 1.4: Considering compounds that have passed the stability test as well as the electronic properties tests, perform extensive defect calculations to determine the *"best-of-class"* candidates.

Outcome of Task 1.4: We have used the Phython code[15] to perform high-throughput calculations for defects on some of the selected halide-Perovskites. This authomated code performs defect calculations and calculates the necessary corrections related to the use of supercells. The formation energy of a defect D (**ΔH)** in the charge state q is a function of the Fermi Energy (E_F) and the elemental chemical potentials (**μ**), and it is given by

$$\Delta H_{\mathrm{D,q}}(E_F,\mu) = [E_{\mathrm{D,q}} - E_{\mathrm{H}}] + \sum_i n_i\mu_i + qE_F + E_{\mathrm{corr}} \quad (1)$$

Here $E_{D,q}$ is the total energy of the supercell with the defect D in charge state q; E_H is the total energy of the supercell without the defects; the second term in the right side of the equation is related to the elemental chemical potential of the exchanged atoms; the third term is related to the electron chemical potential and the last term is related to the finite size corrections.

A detailed description of all corrections can be found in Reference [16]. The main corrections are: potential alignment; image charge correction; band filling and band edge shifts.

One of the main challenges in performing these calculations is related to its comparison to the previous literature, where we can easily find several controversies.[12] For $MAPbI_3$, for instance, we've observed reports showing the existence of deep defects, whereas others only report shallow ones.

There are results in the literature for $CsSnI_3$, but they don't report enough data to guarantee a perfect comparison with our calculations.[17] Our results differ from those in several aspects, including: magnitude of defect formation energies, defect transition energies and order of most stable defects. This strong discrepancy might be because we use larger supercells than those present in the literature, spin polarization and the SCAN functional,[18] that are not used in previous calculations. Recent reports indicate that the use of this functional leads to more precise lattice parameters for Halide Perovskites.[19] Owing to this, we have decided to use this functional as well.

The difficulty in reproducing the results from the literature for $CsSnI_3$ delayed a lot the development of the project. We've started a discussion with the authors of this manuscript in order to understand the difference in the calculations. At the end, we've concluded that those results were not reproducible.

As a *bonus* from the development of this part of the project, we've started a wide discussion with some of the most prominent members of the 'defect calculation community', in order to determine the best practices when performing this type of calculations. This will soon become a manuscript entitled *'Best Practices for Defect Calculations in Semiconductors'*. In the box below, we copy the e-mail that was sent.

E-Mail:

Dear Defect calculation folks,
Distribution list: S.H. Wei; Yanfa Yan, Wan-Jian Yin, Yu Jun Zhao; Stephan Lany; V. Blum; P. Deak; A. Janotti; Mao-Hua Du; Chris Van de walle; Gustavo Dalpian Alex Zunger

Background: There are now quite a few defect and impurity calculations in the literature that gives significantly different results (including deep vs shallow; and high vs low equilibrium concentration of vacancies) even though nominally all such calculations are done with pseudo potential DFT supercells. Such significant differences no longer exist between different first

principles methods for bulk calculations, [Lejaeghere, K. *et al*. *Science* **351**, aad3000 (2016)] but can be severe for defects and doping, where authors often do not state which corrections were applied and which were not, and what's the numerical value of the corrections. This could not only hurt the brand of "first-principles theory of defects", but can also make the all-important experiment-theory interactions highly problematic.

Purpose: The purpose of this community blog is to (1) enlist your support in verifying what a given (published or to be published) defect calculation is actually doing so that each of us could in principle reproduce the results. (2) In the future we would like to strongly recommend that along with publishing papers on defects we should each include a table (attached XLS is a possible sample) that specifies the type of corrections done and their numerical values (see examples below). Although we do not insist on using the same methodology, one wish that what was actually done is clearly and explicitly stated (The CU Boulder group intends from now on to publish as Supporting Information perhaps such a Table for each new system, and we hope others will follow).

To make this very specific, Gustavo Dalpian (dalpian@gmail.com) has worked out 2 systems with defect calculations given below. **It will be great if some volunteers will try and do these independently see if you get similar results to the present benchmark, or to the original papers?**

Please read the attachment

Many Thanks

Alex

Our proposal is that, from point onward, all theoretical papers reporting defect calculations in solids should contain, as supplementary information, a table with all important energies used for the defect calculations. These include: *total energies, band gaps, energy of the valence band maximum, energy of each correction and so on*. Figure 9 reports a sample table with all these energies for $CsSnI_3$. Several of authors that were included in the e-mail list above have already started using the suggested standards. Stephan Lany, in his Physical Review manuscript discussing HSE versus GW calculations for defects;[20] and, Peter Deak used these principles in his manuscript discussing defects in intermediate band compounds.[21]

	A	B	D	E	F	G	H	I	J	K	L	M	N
1		Important parameters for defect calculations.											
2												d_mu (point A)	
3	CsSnI3	orthorombic			Host VBM	2.1448			mu_Sn	-35.886		0	
4					Host CBM	3.0009			mu_I	-37.386667		-0.963666667	
5					epsilon	7.16			mu_Cs	-40.81		-3	
6												mu_CsSnI3	-5.891
7	DEFECT	Charge state	Total Energy	Pot Align	Image corr	Band Filling (VBM)	Band Filling (CBM)	Delta_band	H_f(0)	H_f(CBM)	n_Cs	n_Sn	n_I
8	SC	0	-6042.810246						-0.500	1.356			
9	Sn_I	0	-6038.916	0.006	0.000	0.000	0.000	0.000	2.393	2.393	0	-1	1
10	Sn_I	1	-6041.774	0.017	0.010	0.000	0.000	0.000	1.208	3.064	0	-1	1
11	Sn_I	2	-6044.009	0.026	0.041	0.000	0.000	0.000	0.684	4.396	0	-1	1
12	Sn_I	3	-6046.127	0.040	0.092	0.000	0.000	0.000	0.328	5.896	0	-1	1
13	CsI	0	-6080.558	0.070	0.000	0.000	0.000	0.000	3.062	3.062	-1	0	0
14	CsI	1	-6083.630	0.080	0.010	0.000	0.000	0.000	1.726	3.582	-1	0	0
15	VI	0	-6004.291	-0.025	0.000	0.000	0.000	0.000	1.133	1.133	0	0	1
16	VI	1	-6007.176	-0.020	0.010	0.000	0.000	0.000	-0.117	1.739	0	0	1
17	Cs_Sn	-1	-6044.828	0.011	0.010	0.000	0.000	0.000	1.261	-0.595	-1	1	0
18	Cs_Sn	0	-6046.744	0.007	0.000	-0.227	0.000	0.000	0.763	0.763	-1	1	0
19	SnI	0	-6075.436	0.049	0.000	0.000	0.000	0.000	3.260	3.260	0	-1	0
20	SnI	1	-6077.271	0.050	0.010	0.000	0.000	0.000	3.131	4.987	0	-1	0
21	SnI	2	-6080.182	0.078	0.041	0.000	0.000	0.000	2.002	5.714	0	-1	0
22	II	-1	-6076.814	0.051	0.010	0.000	0.000	0.000	1.698	-0.158	0	0	-1
23	II	0	-6078.693	0.041	0.000	-0.259	0.000	0.000	1.246	1.246	0	0	-1
24	Sn_Cs	0	-6036.760	0.005	0.000	0.000	0.000	0.000	1.126	1.126	1	-1	0
25	Sn_Cs	1	-6039.825	0.009	0.010	0.000	0.000	0.000	-0.275	1.581	1	-1	0
26	VCs	-1	-5999.890	-0.037	0.010	0.000	0.000	0.000	0.513	-1.343	1	0	0
27	VCs	0	-6001.735	-0.046	0.000	-0.253	0.000	0.000	0.013	0.013	1	0	0
28	Cs_I	0	-6043.152	0.018	0.000	0.000	-0.013	0.000	3.068	3.068	-1	0	1
29	Cs_I	1	-6046.220	0.026	0.010	0.000	0.000	0.000	1.695	3.551	-1	0	1
30	Cs_I	2	-6049.258	0.033	0.041	0.000	0.000	0.000	0.372	4.084	-1	0	1
31	I_Sn	-3	-6035.456	-0.026	0.092	0.000	0.000	0.000	4.092	-1.476	0	1	-1
32	I_Sn	-2	-6038.123	-0.001	0.041	0.000	0.000	0.000	2.942	-0.770	0	1	-1
33	I_Sn	-1	-6040.690	0.015	0.010	0.000	0.000	0.000	1.971	0.115	0	1	-1
34	I_Sn	0	-6042.456	0.014	0.000	-0.208	0.000	0.000	1.646	1.646	0	1	-1
35	SC	0	-6042.810	-0.002	0.000	0.000	0.000	0.000	0.000	0.000	0	0	0
36	I_Cs	-2	-6034.533	0.011	0.041	0.000	0.000	0.000	1.584	-2.128	1	0	-1
37	I_Cs	-1	-6035.702	0.004	0.010	0.000	0.000	0.000	2.046	0.190	1	0	-1
38	I_Cs	0	-6037.623	-0.006	0.000	-0.252	0.000	0.000	1.512	1.512	1	0	-1
39	VSn	0	-6006.389	-0.047	0.000	-0.599	0.000	0.000	-0.064	-0.064	0	1	0
40	VSn	-1	-6004.667	-0.047	0.010	-0.201	0.000	0.000	0.469	-1.387	0	1	0
41	VSn	-2	-6002.629	-0.040	0.041	0.000	0.000	0.000	1.127	-2.585	0	1	0

Figure 9. Table reporting total energies and corrections for defect calculations in CsSnI3.

We have studied all intrinsic defects in **$CsSnI_3$, $CsSnBr_3$ and $CsSnCl_3$**. These are Lead-free and stable perovskites with adequate bandgaps for solar cells, and effective masses for PV applications. Besides that, as a bonus, we will be able to track chemical trends as we change the halide atom.

In order to calculate the formation energies, we need to estimate the range of the elemental chemical potentials where the target material is stable. In order to do that, one has to calculate the formation enthalpy of each compound that can be formed by the combination of the constituent atoms. Recent calculations have been using materials repositories in order to get these formation energies. Some of these repositories include the OQMD,[22] the Materials Project[23] and AFLOW.[24] However, as we used the SCAN functional, we have to take this into consideration, re-calculating all stable compounds composed of these elements with the SCAN functional. The databases usually use GGA or GGA+U to perform these calculations. Figure 10 shows the differences between the elemental chemical potentials calculated with the GGA functional and the SCAN functional.

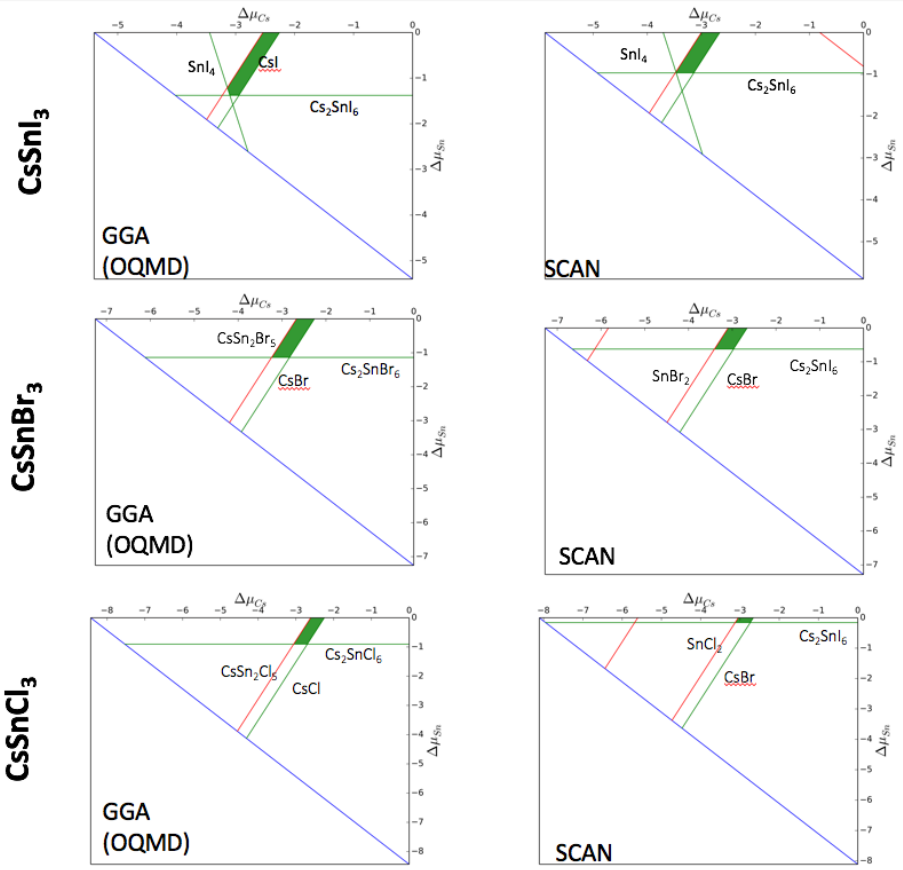

Figure 10. Stability triangles for the studied compounds. The stable area with GGA and with SCAN is similar, although the absolute values of the energies are sligtly different.

Although the 'green' areas in Figure 8, that represent the range of the chemical potentials where the material is stable, are similar for both exchange correlation functionals, it is important to note that the absolute values of the energies are different, what should influence on the absolute values of the formation energies. Also, for $CsSnBr_3$ and $CsSnCl_3$, the limiting compounds are different.

The most important results from our defect calculations are shown in Figure 11, where we report all the formation energies for our target materials. As can be observed, there are no transition levels inside the band gap for the defects with lower formation energies. Exception to interstitial Cl. This should guarantee that $CsSnI_3$ and $CsSnBr_3$ are 'defect tolerant'. The formation energy of the defects can be rather low, what will harm the dopability of these materials: the formation energy of Sn vacancy becomes negative slightly above the VBM, indicating that if the Fermi energy passes this point, defects will spontaneously form, degradation the material. This is an indication that these materials will likely be always p-type.

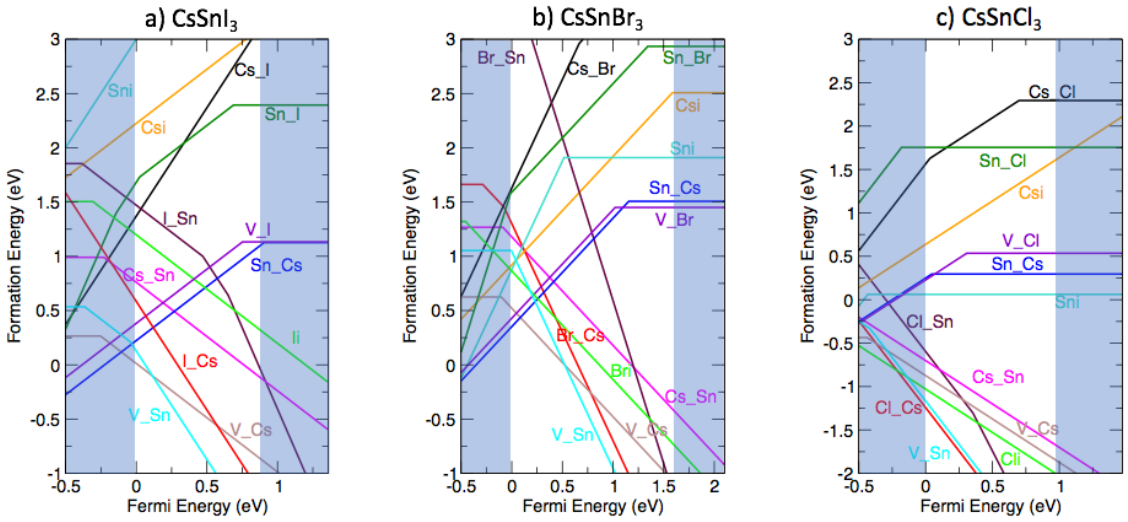

Figure 11. Intrinsic defect formation energy as a function of the Fermi Energy for the studied perovskites. All formation energies were calculated at the Sn-rich chemical environment. The shaded areas represent the valence and conduction bands.

Special attention should be given to CsSnCl3, where several negative formation energies are observed. This occurs because we have decided to use the cubic phase of this compound in the calculations (opposite to I and Br, where the orthorhombic phase was used). As the cubic phase (observed experimentally) is not the lowest energy phase from a theoretical perspective, formation energies become artificially negative.

Owing to the computational costs of the calculations with SCAN, in the results presented above we still don't apply the band edge corrections necessary to predict more carefully the position of transition energies. However, these corrections are continuing, but not under funding for this project.

Task 1.5: Hand off of the most promising (Best-of-Class) results to the appropriate groups for development.

Outcome of Task 1.5:

Our interactions with the perovskite research community continued throughout this project. We have maintained regular communications and exchanges with the major EERE and international groups working in this area including: (1) M. McGehee (Stanford); (2) Stephan Lany and J. Berry (NREL); (3) Y. Yan (Univ. of Toledo); (4) David Mitzi (Duke University); (5) M. Grätzel (PFUL); (6) H. Snaith (Univ. of Oxford); (7) Hemamala Karunadasa (Stanford University); (8) M.G. Kanatzidis and C. Stroumpos (Northwestern University); (9) Anil Kottantharayil (IIT-Bombay India); (9) Su-huai Wei (Beijing Computational Science Research Center, China)

During this time, the University of Colorado added M. McGehee to its staff, providing for closer/immediate interactions and exchanges between our theory work and the needs of the experimentalists.

We have had many discussions at major science conferences: IEEE PVSC, APS March Meeting, Oxford Special Meeting on Perovskites, National Academy of Science.

These interactions have resulted in several publications (Section 7). A major highlight is the development of the working blog on defects that was described under Task 1.4. This is a major activity that continues—and is expanding in its participation.

The DOE Special Poster Session held at the IEEE PVSC (Washington, DC, June 2017) was a very significant event that helped bring the EERE research community funded in the PV area together. It provided a very useful platform to interact with all the funded research under the DOE EERE program on these perovskite materials and solar cells.

4. Conclusions

We have identified in this materials screening program 18 winning compounds from a materials space composed of ~100 candidates, including the most commonly used materials of $[CH_3NH_3]PbI_3$ and $[CH(NH_2)_2]PbI_3$. Of them 14 are Pb-free (including 5 Ge-based materials, i.e., CsGeI3, CsGeBr3, [NH3OH]GeBr3, $[NH_2NH_3]GeBr_3$, and $[CH_3NH_3]GeI_3$, and 9 Sn-based materials, i.e., $CsSnI_3$, $CsSnBr_3$, $CsSnCl_3$, $[CH_3NH_3]SnI_3$, $[CH_3NH_3]SnBr_3$, $[CH(NH_2)_2]SnI_3$, $[CH_3CH_2NH_3]SnI_3$, $[C(NH_2)_3]SnI_3$, and $[NH_2(CH_3)_2]SnI_3$), and 7 show substantially enhanced thermodynamic stability with respect to $[CH_3NH_3]PbI_3$ (i.e., $CsSnBr_3$, $CsSnCl_3$, $CsGeBr_3$, $[CH_3NH_3]SnI_3$, $[CH_3NH_3]SnBr_3$, $[CH_3CH_2NH_3]SnI_3$, and $[NH_2(CH_3)_2]SnI_3$).

Our defect calculations focused $CsSnI_3$, $CsSnBr_3$ and $CsSnCl_3$, and we have found that they should be defect tolerant, i.e., do not present transition levels inside the band gap. Also, Sn vacancies have low formation energies, becoming negative at energies slightly above the VBM. Because of this, they should be usually p-type semiconductors. As an enhancement (a ‘bonus’), we have also started a discussion (see Section 3, Task 1.4) on the ‘defects’ community stating best practices when performing defect calculations in solids. This discussion blog will continue (though this project is completed) because of the importance of these interactions to the development of these solar cell types and to ensuring the accuracy of our defect results.

5. Budget and Schedule:

Budget Period 1 was in effect initially from 07/01/2016 through 06/30/2017 subsequent to a large delay in the processing of the award documents. As a result of this delay, the Project Team received pre-award authorization to begin work on 04/01/2016. Later, a no-cost extension was approved through 12/31/2017. The Federal share was awarded for $225,000 and the non-Federal share was negotiated at 10% of total project costs, or $25,000. All funds have been spent as of 12/31/2017. Actual expenses did not deviate significantly from the spending plan. Dr. Y. Yu accepted another position prior to the start date and was replaced by Visiting Professor Gustavo Dalpian. Personnel costs, in any event, deviated less than 4% from that originally budgeted.

6. Path Forward

We have recently approved another SIPS grant that will be used to conduct a research on perovskite alloys (DE-EE-0008153 (PVRD2) – Title: *Isovalent alloying and heterovalent substitution as routes to accelerate the development and optimization of super-efficient halide perovskite PV solar cells*). Consequently, our work on perovskites will be continued, and there will be some relationship between the two projects. What has been learned in the current proposal will be used in the next one, and we continue our interactions and collaborations with other groups in this research area.

This path forward addresses the next requirements to bring the perovskites toward optimal performance and manufacturing. First generation hybrid-perovskite (RUNG 1) solar cells have been prepared by individual single-perovskite halide components such as $APbI_3$, $ASnI_3$, $APbBr_3$, $ASnBr_3$ with different A cations, such as methylammonium (MA) with formamidinium (FM). RUNG 2 is obtained by mixing B cations (Sn and Pb), and X anions (Cl and Br or I) producing a disordered alloy (A, A')(M,M')(X,X')3Vspace. The most advanced RUNG 3 corresponds to heterovalentVsubstitution of halide perovskites, creating an ordered double-perovskite compound. This path forward builds upon RUNG 1 knowledge and construct first-principles understanding, design, optimization, and validation of (RUNG 2) isovalent halide perovskite alloys, and (RUNG 3) heterovalentVsubstitution of halide perovskites. These second and third rungs, respectively, in the ladder of perovskite research have extremely high potential for significant improvements and innovative discoveries in this field.

We have two additional manuscripts that are in process. These major topics for these are: (1) discussing the 'best practices' when performing defect calculations in solids, and (2) other discussing the specific case of defects and doping in the halide perovskites. These two papers are under review. These will be provided to the DOE managers when they are accepted.

7. Publications Resulting from This Work:

a. D. Yang, X. Zhao, Q. Xu, Y. Fu, Y. Zhan, Alex Zunger, and Lijun Zhang, "Functionality-Directed Screening of Pb-Free Hybrid Organic−Inorganic Perovskites with Desired Intrinsic Photovoltaic Functionalities," Chemistry of Materials 29, 524 (2017).

a. Lijun Zhang, D. Yang, Jian Lv, X. Zhao, J.H. Yang, Liping Yu, Su-Huai Wei, and Alex Zunger, "Design of Lead-free Halide Perovskites for Solar Cells via Photovoltaic-functionality-directed Materials," Presented at the March Meeting, American Physical Society (2017).

b. Gustavo M. Dalpian, Qihang Liu, Constantinos C. Stoumpos, Alexios P. Douvalis, Mahalingam Balasubramanian, Mercouri G. Kanatzidis, and Alex Zunger Phys. Rev. Materials 1, 025401 (2017)

c. Alex Zunger, G. Dalpian, Qihang Liu, L.B Abdalla, and L.L. Kazmerski, "Developing an Understanding-Based Selection of Hybrid-Perovskite Compounds and the Cu-In Hybrid-Perovskite (CIHP) Family", Proceedings of the 44th IEEE Photovoltaic Specialists Conference, Washington, DC (June 2017) (invited). (Highlighted as one of the most significant paper contributions to the 44th IEEE Photovoltaic Specialists Conference – IEEE PVSC.)

d. Alex, Zunger, G. Dalpian, L.B. Abdalla, and L.L. Kazmerski, "Theoretical design and discovery of the most-promising, previously overlooked hybrid perovskite compounds", Special DOE Poster Session on Research, IEEE Photovoltaic Specialists Conference, Washington, DC, June 2017.

e. Alex Zunger. Physics Next meeting June 2017, Long Island, NY (organized by APS and PRX, PRL): Invited talk on materials-by-design with emphasis on halide perovskite

f. Alex Zunger. National Academy of Science presentation on "Future of Materials Science," Golden, Colorado, July 27: Invited talk on designer electronic materials.

g. Alex Zunger. Plenary talk at the Oxford Meeting on halide perovskites (September/2017)

8. References:

1 Kojima, A.; Teshima, K.; Shirai, Y.; Miyasaka, T. Organometal Halide Perovskites as Visible-Light Sensitizers for Photovoltaic Cells. Journal of the American Chemical Society 2009, 131, 6050–6051.

2 Eperon, G. E.; Leijtens, T.; Bush, K. A.; Prasanna, R.; Green, T.; Wang, J. T.-W.; McMeekin, D. P.; Volonakis, G.; Milot, R. L.; May, R.; et al. Perovskite-Perovskite Tandem Photovoltaics with Optimized Band Gaps. Science 2016, 354, 861–865.

3 Bush, K. A.; Palmstrom, A. F.; Yu, Z. J.; Boccard, M.; Cheacharoen, R.; Mailoa, J. P.; McMeekin, D. P.; Hoye, R. L. Z.; Bailie, C. D.; Leijtens, T.; et al. 23.6%-Efficient Monolithic Perovskite/Silicon Tandem Solar Cells with Improved Stability. Nature Energy 2017, 2, 17009.

4 Bi, C.; Chen, B.; Wei, H.; DeLuca, S.; Huang, J. Efficient Flexible Solar Cell Based on Composition-Tailored Hybrid Perovskite. Advanced Materials 2017, 29, 1605900.

5 Ergen, O.; Gilbert, S. M.; Pham, T.; Turner, S. J.; Tan, M. T. Z.; Worsley, M. A.; Zettl, A. Graded Bandgap Perovskite Solar Cells. Nature Materials 2016, 16, 522–525.

6 Prasanna, R.; Gold-Parker, A.; Leijtens, T.; Conings, B.; Babayigit, A.; Boyen, H.-G.; Toney, M. F.; McGehee, M. D. Band Gap Tuning via Lattice Contraction and Octahedral Tilting in Perovskite Materials for Photovoltaics. Journal of the American Chemical Society 2017, 139, 11117–11124.

7 Yang, Y.; You, J. Make Perovskite Solar Cells Stable. Nature 2017, 544, 155–156.

8 Zhao, X.-G.; Yang, D.; Sun, Y.; Li, T.; Zhang, L.; Yu, L.; Zunger, A. Cu–In Halide Perovskite Solar Absorbers. Journal of the American Chemical Society 2017, 139, 6718–6725.

9 Volonakis, G.; Haghighirad, A. A.; Milot, R. L.; Sio, W. H.; Filip, M. R.; Wenger, B.; Johnston, M. B.; Herz, L. M.; Snaith, H. J.; Giustino, F. Cs2InAgCl6: A New Lead-Free Halide Double Perovskite with Direct Band Gap. The Journal of Physical Chemistry Letters 2017, 8, 772–778.

10 Walsh, A.; Zunger, A. Instilling Defect Tolerance in New Compounds. Nature Materials 2017, 16, 964–967.

11 Yin, W.-J.; Shi, T.; Yan, Y. Unusual Defect Physics in CH3NH3PbI3 Perovskite Solar Cell Absorber. Applied Physics Letters 2014, 104, 63903.

12 Du, M.-H. Density Functional Calculations of Native Defects in CH3NH3PbI3: Effects of Spin–Orbit Coupling and Self-Interaction Error. The Journal of Physical Chemistry Letters 2015, 6, 1461–1466.

13 G. P. Nagabhushana, Radha Shivaramaiah, and Alexandra Navrotsky, PNAS 113, 7717 (2016)

14 Z. Xiao, Y. Zhou, H.Hosono, and T. Kamiya, PCCP 17, 18900 (2015).

15 Goyal, A.; Gorai, P.; Peng, H.; Lany, S.; Stevanović, V. A Computational Framework for Automation of Point Defect Calculations. Computational Materials Science 2017, 130, 1–9.

16 Lany, S.; Zunger, A. Assessment of Correction Methods for the Band-Gap Problem and for Finite-Size Effects in Supercell Defect Calculations: Case Studies for ZnO and GaAs. Physical Review B 2008, 78.

17 Xu, P.; Chen, S.; Xiang, H.-J.; Gong, X.-G.; Wei, S.-H. Influence of Defects and Synthesis Conditions on the Photovoltaic Performance of Perovskite Semiconductor CsSnI3. Chemistry of Materials 2014, 26, 6068–6072.

18 Sun, J.; Remsing, R. C.; Zhang, Y.; Sun, Z.; Ruzsinszky, A.; Peng, H.; Yang, Z.; Paul, A.; Waghmare, U.; Wu, X.; et al. Accurate First-Principles Structures and Energies of Diversely Bonded Systems from an Efficient Density Functional. Nature Chemistry 2016, 8, 831–836.

19 Bokdam, M.; Lahnsteiner, J.; Ramberger, B.; Schäfer, T.; Kresse, G. Assessing Density Functionals Using Many Body Theory for Hybrid Perovskites. Physical Review Letters 2017, 119.

20 Peng, H.; Scanlon, D. O.; Stevanovic, V.; Vidal, J.; Watson, G. W.; Lany, S. Addendum to “Convergence of Density and Hybrid Functional Defect Calculations for Compound Semiconductors.” Physical Review B 2017, 96.

21 Han, M.; Zeng, Z.; Frauenheim, T.; Deák, P. Defect Physics in Intermediate-Band Materials: Insights from an Optimized Hybrid Functional. Physical Review B 2017, 96.

22 http://oqmd.org/

23 https://materialsproject.org/

24 http://aflowlib.org/